

**Gold-catalyzed thioetherification of allyl, benzyl, and propargyl phosphates**

|                               |   |
|-------------------------------|---|
| Journal:                      | <i>Catalysis Science &amp; Technology</i>   |
| Manuscript ID                 | CY-ART-11-2021-002085.R2  |
| Article Type:                 | Paper   |
| Date Submitted by the Author: | 08-Jan-2022   |
| Complete List of Authors:     | Miura, Hiroki; Tokyo Metropolitan University, Department of Applied Chemistry for Environment, Graduate School of Urban Environmental Sciences<br>Toyomasu, Tomoya; Tokyo Metropolitan University, Department of Applied Chemistry for Environment, Graduate School of Urban Environmental Sciences<br>Nishio, Hidenori; Tokyo Metropolitan University, Department of Applied Chemistry for Environment, Graduate School of Urban Environmental Sciences<br>Shishido, Tetsuya; Tokyo Metropolitan University, Applied Chemistry for Environment |
|                               |   |

## ARTICLE

# Gold-catalyzed thioetherification of allyl, benzyl, and propargyl phosphates†

Hiroki Miura<sup>\*abc</sup>, Tomoya Toyomasu<sup>a</sup>, Hidenori Nishio<sup>a</sup> and Tetsuya Shishido<sup>\*abc</sup>

Received 00th January 20xx,  
Accepted 00th January 20xx

DOI: 10.1039/x0xx00000x

Gold-catalyzed thioetherification of C(sp<sup>3</sup>)-O bonds is described. The reaction of allyl phosphates and thiosilanes in the presence of gold nanoparticles supported on ZrO<sub>2</sub> proceeded efficiently under mild reaction conditions to give the corresponding allyl sulfides in excellent yields. ZrO<sub>2</sub>-supported gold nanoparticles showed excellent catalytic turnover and reusability. In addition, the C-O bonds of benzyl and propargyl phosphates underwent thioetherification to afford benzyl and propargyl sulfides. The reaction of an optically active benzyl phosphate proceeded with excellent chirality transfer to give a benzyl sulfide with high enantiomeric purity. Control experiments corroborated that soluble gold species were responsible for the efficient thioetherification of C-O bonds of phosphates, and characterization of the catalysts revealed that cationic gold species at the surface of gold nanoparticles supported on ZrO<sub>2</sub> served as a source for highly active catalytic species.

## Introduction

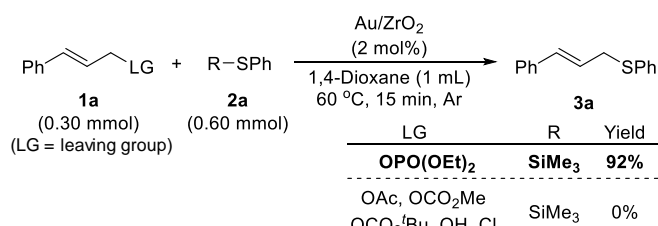
Organo sulfur compounds are important in organic synthesis, chemical biology and materials science.<sup>1</sup> Thus, tremendous effort has been devoted to the development of efficient method of C-S bond formation.<sup>2-7</sup> Particularly, allyl, benzyl and propargyl sulfides are often used as substrates for synthesizing value-added organic molecules.<sup>8-10</sup> Treatment of carbon electrophiles, such as allyl halides, with thiols as sulfur nucleophiles under basic conditions is one of the most convenient approaches for the formation of C-S bonds.<sup>11,12</sup> However, this method is limited to thioetherification at primary carbons. In contrast, transition-metal catalysts make it possible for thioetherification to occur at secondary and tertiary carbons. Furthermore, they allow alcohols and their ester derivatives to participate in thioetherification. Activation of C(sp<sup>3</sup>)-O bonds by Lewis acid catalysts has been reported to be one of the most effective methods for the efficient thioetherification of C(sp<sup>3</sup>)-O bonds. In this regard, Fe,<sup>13,14</sup> Ni,<sup>15</sup> Ru,<sup>16-20</sup> Pd,<sup>21-30</sup> In,<sup>31,32</sup> Ir,<sup>33-35</sup> Au,<sup>36</sup> and lanthanoides<sup>37</sup> have all been reported to be efficient catalysts for thioetherification of C(sp<sup>3</sup>)-O bonds. On the other hand, supported metal nanoparticle (NP) catalysts have attracted considerable attention since they facilitate the recycling of precious metals and reduce contamination of products from metallic loads. Au

NP catalysts have been reported to promote various organic reactions as a result of

their Lewis acidic character.<sup>38</sup> In the course of our studies on the catalytic effects of Au NPs toward carbon-heteroatom bond formation,<sup>39</sup> we developed an efficient borylation of C(sp<sup>3</sup>)-O bonds of allyl, benzyl and propargyl esters in the presence of supported Au catalysts.<sup>40</sup> This result inspired us to develop further applications of Au NP catalysts to the nucleophilic substitution of carbon electrophiles. Herein, we report the thioetherification of C(sp<sup>3</sup>)-O bonds by supported Au catalysts. Au NPs supported on ZrO<sub>2</sub> efficiently catalyzed the thioetherification of allyl-, benzyl- and propargyl phosphates to give the corresponding sulfides. Detailed control experiments and characterization of catalysts revealed that soluble Au species are responsible for the efficient C-S bond formation, and cationic gold species at the surface of gold nanoparticles supported on ZrO<sub>2</sub> served as a source for highly active catalytic species.

## Results and discussion

First, we investigated the thioetherification of allylic electrophiles in the presence of ZrO<sub>2</sub>-supported Au catalyst (Scheme 1). The reaction of cinnamyl phosphate (**1a**) and phenyl(trimethylsilyl)sulfane (**2a**) in 1,4-dioxane gave the corresponding cinnamylsulfanylbenzene (**3a**) in 92% yield. The use of phosphate as a leaving group is crucial, and no C-S



Scheme 1. Au/ZrO<sub>2</sub>-catalyzed allylic thioetherification.

<sup>a</sup> Department of Applied Chemistry for Environment, Graduate School of Urban Environmental Sciences, Tokyo Metropolitan University, 1-1 Minami-Osawa, Hachioji, Tokyo 192-0397, Japan.

<sup>b</sup> Research Center for Hydrogen Energy-based Society, Tokyo Metropolitan University, 1-1 Minami-Osawa, Hachioji, Tokyo 192-0397, Japan.

<sup>c</sup> Element Strategy Initiative for Catalysts & Batteries, Kyoto University, Katsura, Nishikyo-ku, Kyoto 615-8520, Japan.

† Electronic Supplementary Information (ESI) available. See DOI: 10.1039/x0xx00000x

coupling took place in the reaction of cinnamyl acetate, carbonate, alcohol and chloride with Au/ZrO<sub>2</sub> catalyst. Furthermore, in sharp contrast to the high reactivity of thiosilane for the present Au-catalyzed C–S coupling, thiol was not suitable as a sulfur nucleophile.

The effects of metal nanoparticles and the type of support on the reactions of **1a** and **2a** are shown in Table 1. In addition to Au catalyst (entry 1), Ag and Cu catalysts showed moderate activity (entries 2 and 3). On the other hand, the reaction with Pd, Rh and Pt catalysts resulted in a low yield of **3a** (entries 4–6). The type of support remarkably affected the performance of Au catalysts, and CeO<sub>2</sub>-supported Au catalyst showed comparable activity to Au/ZrO<sub>2</sub> (entry 7). In contrast, TiO<sub>2</sub>, Al<sub>2</sub>O<sub>3</sub> and SiO<sub>2</sub> were found to be unsuitable supports for the reaction (entries 8–10). Although primary allylic electrophiles have been reported to undergo thioetherification under basic conditions, the surface basicity of ZrO<sub>2</sub> was not sufficient to promote the reaction efficiently (entry 11), indicating that Au species are an essential catalytic component for the present C–S coupling. On the other hand, cationic Au complex exhibited high catalytic activity to give **3a** in 88% yield (entry 12). Furthermore, Au/ZrO<sub>2</sub> catalyst that had been calcined in air at 500 °C before the reaction showed no activity for C–S coupling (entry 13). Since

oxidative treatment at high temperature promotes the reduction of Au species, cationic gold species should be responsible for efficient catalytic C–S bond formation. The high catalytic activity of Au/ZrO<sub>2</sub> was reflected in the reaction with a quite low catalyst loading, and the catalytic turnover number (TON) reached 8700 in the reaction with 0.01 mol% Au/ZrO<sub>2</sub> (entry 14). This TON value was much higher than that recorded with Me<sub>2</sub>SAuCl catalyst (entry 15), which proving superior catalytic activity of Au/ZrO<sub>2</sub>. Moreover, Au/ZrO<sub>2</sub> could be used for the gram-scale synthesis of **3a** under mild reaction conditions (entry 16). Unfortunately, simple alkyl phosphates, such as diethyl octyl phosphate and diethyl phenethyl phosphate did not undergo thioetherification under the present Au catalysis.

With the optimized catalyst in hand, the scope of allyl phosphates in the supported Au-catalyzed thioetherification was investigated (Table 2). The reactions of primary allyl phosphates provided the corresponding allyl sulfides (**3b–3e**) in high yields. Note that the *E/Z* configuration at the alkene moiety of terpene-based compounds was completely maintained during the catalytic reactions. The Au-catalyst also efficiently catalyzed double-thioetherification of bisphosphate **1f** to give

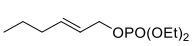
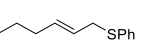
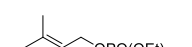
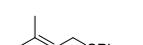
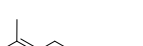
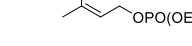
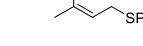
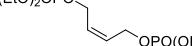
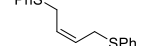
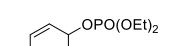
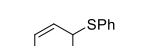
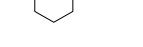
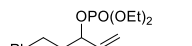
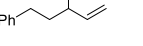
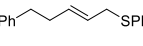
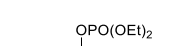
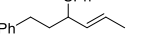
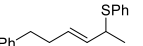
**Table 1.** Effect of catalysts<sup>a</sup>

| Entry | Catalyst                                     | Yield (%) <sup>b</sup>                 |
|-------|--|--|
| 1     | Au/ZrO <sub>2</sub>                          | 92                                     |
| 2     | Ag/ZrO <sub>2</sub>                          | 71                                     |
| 3     | Cu/ZrO <sub>2</sub>                          | 27                                     |
| 4     | Pd/ZrO <sub>2</sub>                          | 7                                      |
| 5     | Rh/ZrO <sub>2</sub>                          | 5                                      |
| 6     | Pt/ZrO <sub>2</sub>                          | 0                                      |
| 7     | Au/CeO <sub>2</sub>                          | 86                                     |
| 8     | Au/TiO <sub>2</sub>                          | 22                                     |
| 9     | Au/Al <sub>2</sub> O <sub>3</sub>            | 16                                     |
| 10    | Au/SiO <sub>2</sub>                          | 0                                      |
| 11    | ZrO <sub>2</sub>                             | 4                                      |
| 12    | Me <sub>2</sub> SAuCl                        | 88                                     |
| 13    | Au/ZrO <sub>2</sub> <sup>c</sup>             | 1                                      |
| 14    | Au/ZrO <sub>2</sub><br>(0.01 mol%, 20 h)     | 87<br>(TON = 8700)                     |
| 15    | Me <sub>2</sub> SAuCl<br>(0.02 mol%, 20 h)   | 26<br>(TON = 1300)                     |
| 16    | Au/ZrO <sub>2</sub><br>( <b>1a</b> : 6 mmol) | (75) <sup>d</sup><br>(1.03 g isolated) |

<sup>a</sup> Reaction conditions: **1a** (0.30 mmol), **2a** (0.6 mmol), catalyst (2.0 mol% as metal), 1,4-dioxane (1.0 mL), at 60 °C for 15 min.

<sup>b</sup> Yields were determined by GC analysis by using biphenyl as internal standard. <sup>c</sup> Calcined in air at 500 °C. <sup>d</sup> Isolated yield.

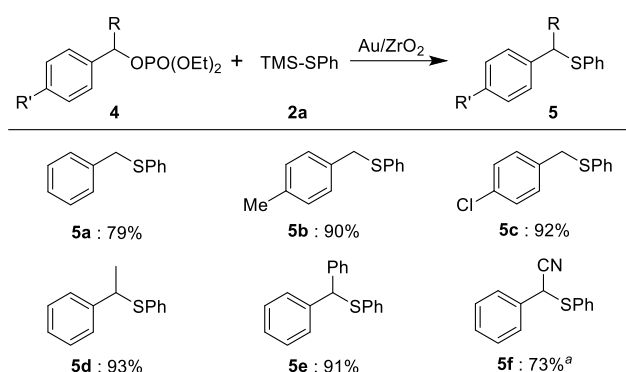
**Table 2.** Scope of allyl phosphates for thioetherification over Au/ZrO<sub>2</sub><sup>a</sup>

| Entry | Substrate  | Product  | Yield [%]         |
|-------|--|--|-------------------|
| 1     |  |   | 99                |
| 2     |  |   | 74                |
| 3     |  |   | 94                |
| 4     |  |   | 94                |
| 5     |  |   | 91                |
| 6     |  |   | 86                |
| 7     |  | <br> | 90<br>(α:γ=36:64) |
| 8     |  | <br> | 93<br>(α:γ=51:49) |
| 9     |  | <br> | 74<br>(α:γ=54:46) |

<sup>a</sup> Reaction condition: **1** (0.3 mmol), **2a** (0.6 mmol), Au/ZrO<sub>2</sub> (2 mol%), 1,4-dioxane (1.0 mL), 60 °C, 30 min, under Ar. Isolated yields are shown.

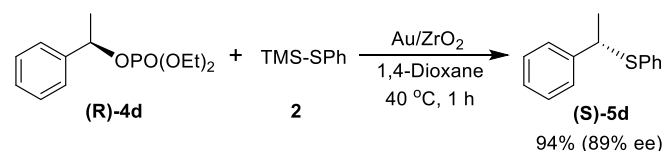
**3f** in 91% yield. Furthermore, Au/ZrO<sub>2</sub> catalyst made it possible to insert thiophenyl groups at secondary carbons. Cyclohexenyl phosphate underwent thioetherification to afford **3g** in 86% yield. On the other hand, thioetherification of secondary allyl phosphate **1h** took place not only at an  $\alpha$ -position but also at a  $\gamma$ -position to form a mixture of regioisomers **3h- $\alpha$**  and **3h- $\gamma$** , where thioetherification occurred preferentially at a terminal position. While equivalent amounts of regioisomers were obtained, the substituent introduced at an alkene moiety did not reduce the yield of the product (**3i** and **3j**).

The Au/ZrO<sub>2</sub> catalyst was also effective for benzylic thioetherification (Scheme 2). The reaction of benzyl phosphate (**4a**) with **2a** afforded benzyl sulfide **5a** in 79% yield. The electronic effect of methyl and chloro groups at the para position of the phenyl ring were not significant, and the corresponding benzyl sulfides (**5b** and **5c**) were obtained in respective yields of 90% and 92%. Furthermore, Au/ZrO<sub>2</sub> catalyst was also effective for the thioetherification of secondary benzyl phosphates, and both alkyl and aryl groups were compatible as second substituents at the benzylic position to give benzyl sulfides (**5d** and **5e**) in excellent yields. In addition, an electrophilic cyano group was tolerated during Au-catalyzed C–S bond formation to give cyano sulfide (**5f**) in 73% yield.



### Scheme 2. Thioetherification of benzyl phosphates over Au/ZrO<sub>2</sub><sup>a</sup>

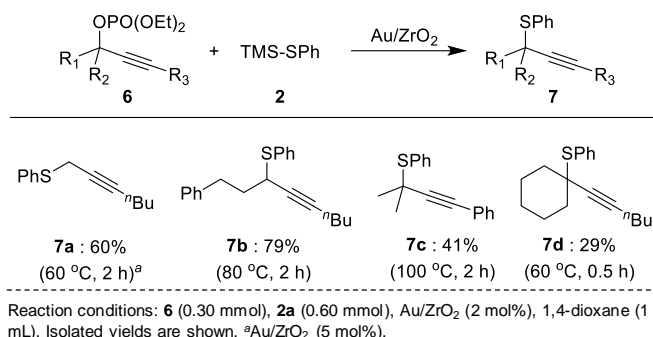
Next, we examined the chirality transfer of optically enriched benzyl phosphates. To our delight, the reaction of (**R**)-**4d** and **2a** proceeded stereospecifically to afford benzyl sulfide (**S**)-**5d** in 94% yield and 89% ee (Scheme 3). This result allows us to deduce that the thioetherification of C–O bonds by Au catalysts proceeds via S<sub>N</sub>2-type mechanism.



### Scheme 3. Chirality transfer in the thioetherification of secondary benzyl phosphate ((**R**)-**4d**) over Au/ZrO<sub>2</sub> Catalyst.

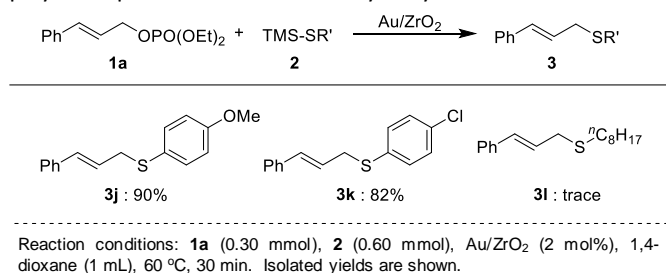
Furthermore, propargyl sulfides could be synthesized by Au-catalyzed thioetherification (Scheme 4). Primary and secondary propargyl phosphates participated in the present C–S coupling to give the corresponding propargyl sulfides **7a** and **7b** in

respective yields of 60% and 79%. Furthermore, Au/ZrO<sub>2</sub> catalyst was effective for the synthesis of tertiary propargyl sulfides **7c** and **7d**. We previously reported that Au/TiO<sub>2</sub> catalyst showed high activity for the borylation of propargyl carbonates to give allenyl boronates.<sup>40</sup> In contrast, the present thioetherification took place exclusively at C–O bonds, and no allenyl sulfides were formed.



### Scheme 4. Thioetherification of propargyl phosphates over Au/ZrO<sub>2</sub> Catalyst

The scope of thiosilanes was also investigated (Scheme 5). The reaction of aryl(trimethylsilyl)sulfanes proceeded efficiently to give **3b** and **3c** in respective yields of 90% and 82%. In contrast, thiosilane with an alkyl group did not participate in the Au-catalyzed C–S coupling, which implies that an aryl group would play an important role in the catalytic cycle.



### Scheme 5. Scope of thiosilane

The reusability of Au/ZrO<sub>2</sub> catalyst for the thioetherification of both primary and secondary allylic phosphates (**1a** and **1f**) was examined. As shown in Fig. 1, the solid Au/ZrO<sub>2</sub> catalyst could



Reaction conditions: **1a** or **1f** (0.6 mmol), **2a** (1.2 mmol), Au/ZrO<sub>2</sub> (2.0 mol%), 1,4-dioxane (2 mL), 60 °C, 15 min. Yields were determined by GC.

### Fig. 1. Reusability of Au/ZrO<sub>2</sub> catalyst for allylic thioetherification.

be used repeatedly for the thioetherification of both primary and secondary allyl phosphates (**1a** and **1f**) at least five times without a significant reduction in the yields of **3a** and **3f**. Since Au/ZrO<sub>2</sub> shows high catalytic turnover and enables gram-scale synthesis in the title reaction (Table 1, entries 15 and 17), the present catalytic system should be suitable requirement for the practical synthesis of thioethers.

To gain further information about the nature of the catalytically active species, the effect of the removal of solid catalyst by hot filtration through a PTFE filter (pore size 0.45 μm) was investigated. Figure 2 shows the time course of the reaction with and without removal of the solid catalyst. Although hot filtration of the solid catalyst slowed the reaction rate, the yield of the product continuously increased. Atomic absorption spectroscopy estimated that 6.7% of total Au species was contained in the filtrate. This result suggests that soluble gold species mainly functioned as an active catalyst for the present thioetherification and that the support might dominate the degree of leaching of Au species from nanoparticles.

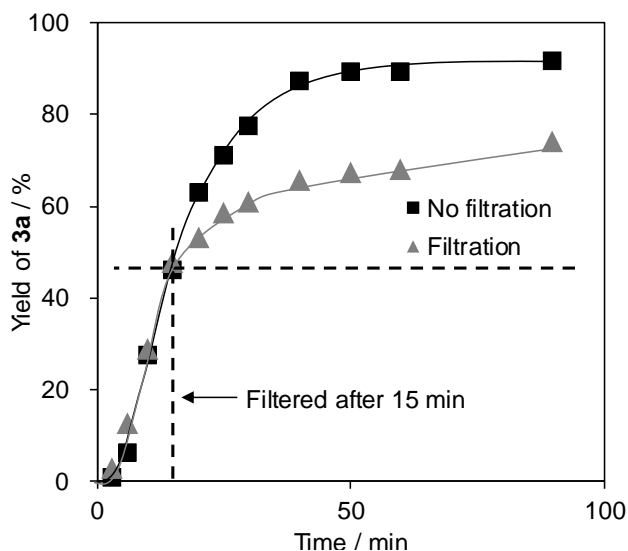
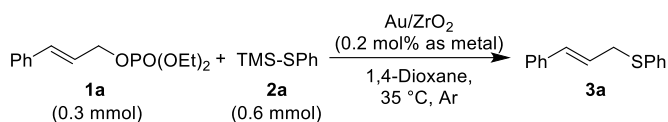


Fig. 2. Hot filtration of Au/ZrO<sub>2</sub> catalysts.

As shown in Table 1, the effect of the support on the performance of supported Au catalyst was remarkable. TEM images of supported Au catalysts and their average particle size are summarized in Fig. 3. Partial aggregation and poor size-regulation of Au NPs were seen in SiO<sub>2</sub>- and Al<sub>2</sub>O<sub>3</sub>-supported Au catalysts (Fig. 3-b and d), which suggests that the high dispersity of Au NPs is important for high catalytic performance toward C-S coupling. On the other hand, although Au/TiO<sub>2</sub> catalysts showed much lower activity than Au/ZrO<sub>2</sub> for the reaction, the size and regulation of Au NPs on TiO<sub>2</sub> were similar to those on ZrO<sub>2</sub> (Fig. 3-a and c). Although a clear image of Au NPs on CeO<sub>2</sub> could not be obtained due to poor contrast of Ce and Au, the absence of peaks that could be attributed to crystalline Au NPs in the XRD pattern of Au/CeO<sub>2</sub> indicates the presence of highly

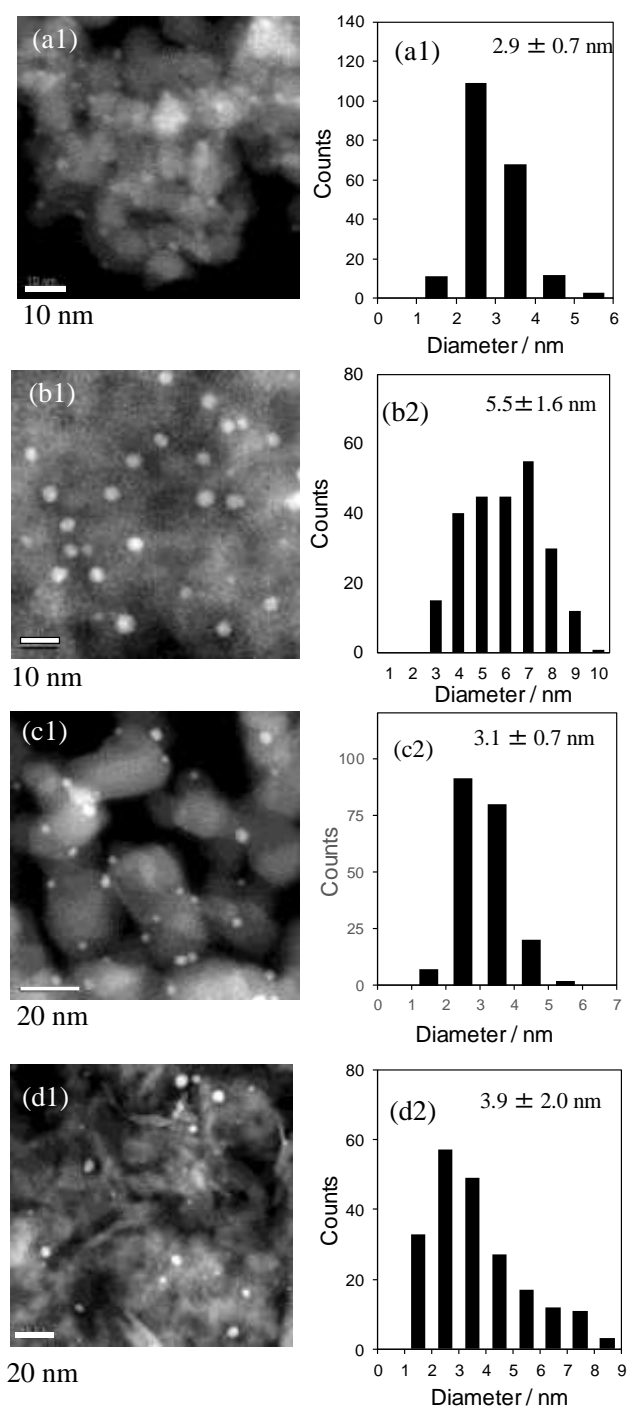
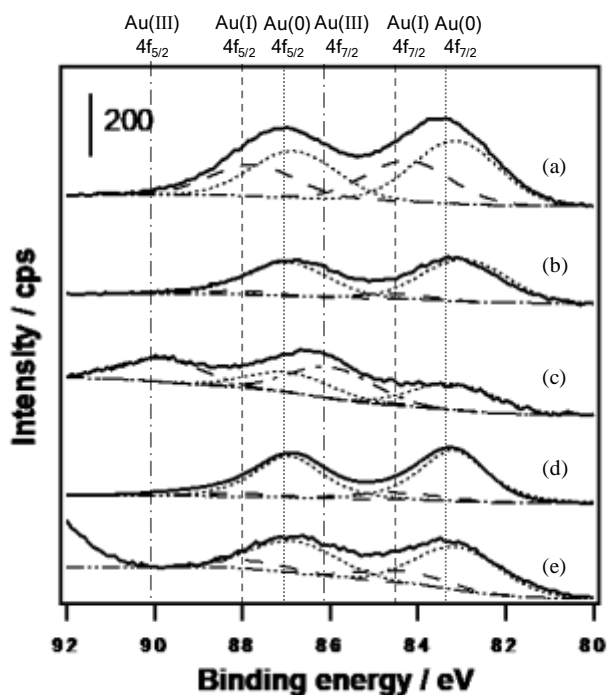


Fig. 3. HAADF-STEM images of supported Au catalysts (a1) Au/ZrO<sub>2</sub>, (b1) Au/SiO<sub>2</sub>, (c1) Au/TiO<sub>2</sub>, (d1) Au/Al<sub>2</sub>O<sub>3</sub>, and (a2–d2) their particle size distribution histograms.

dispersed Au NPs on CeO<sub>2</sub> (See Supplementary Information). These observations imply that some factor other than size and the regulation of Au NPs could be crucial for determining the catalytic performance toward the C–S bond formation.

XPS analysis of supported Au catalysts was carried out to evaluate the electronic state of Au species (Fig. 4). Metallic gold has been reported to be thermodynamically more stable than gold cations at high temperatures. Thus, spontaneous decomposition of gold cation to metallic gold can occur at high



Original spectra (—), Au(0) (.....), Au(I) (---), Au(III) (---)

**Fig. 4.** XP spectra around the Au 4f states of (a) Au/ZrO<sub>2</sub> calcined at 300 °C, (b) Au/ZrO<sub>2</sub> calcined at 500 °C, (c) Au/CeO<sub>2</sub>, (d) Au/TiO<sub>2</sub>, and (e) Au/SiO<sub>2</sub>.

temperatures.<sup>41–44</sup> Curve-fitting analysis of XP spectra revealed that both Au(0) and Au(I) species were present at the surface of Au/ZrO<sub>2</sub> catalyst calcined at 300 °C (Table 3). In contrast, cationic Au species were almost completely absent from the XP spectrum of Au/ZrO<sub>2</sub> catalyst calcined at 500 °C which showed

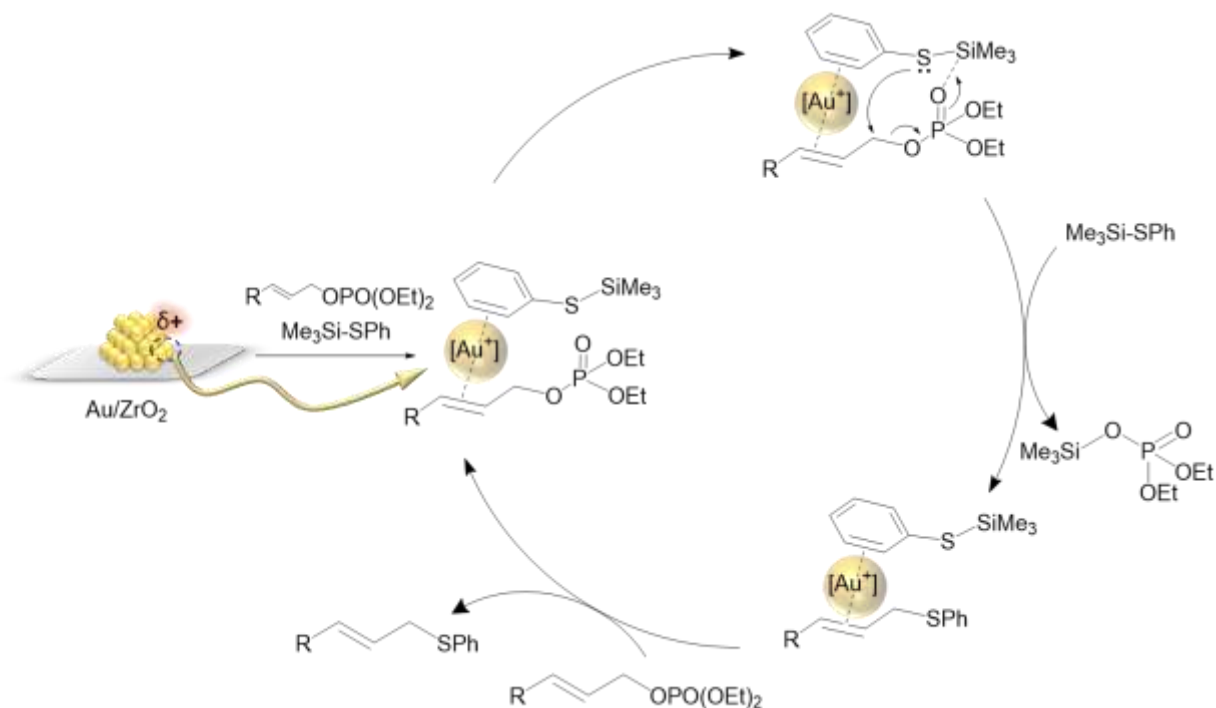
**Table 3.** Fraction of Au species at the surface of supported Au catalysts estimated by XPS curve-fitting analysis.

| Catalyst                         | Au(0)<br>(%) | Au(I)<br>(%) | Au(III)<br>(%) |
|----------------------------------|--------------|--------------|----------------|
| Au/ZrO <sub>2</sub> <sup>a</sup> | 57           | 43           | 0              |
| Au/ZrO <sub>2</sub> <sup>b</sup> | 95           | 5            | 0              |
| Au/CeO <sub>2</sub>              | 44           | 4            | 52             |
| Au/TiO <sub>2</sub>              | 87           | 13           | 0              |
| Au/SiO <sub>2</sub>              | 80           | 20           | 0              |

<sup>a</sup>Calcined at 300 °C. <sup>b</sup>Calcined at 500 °C.

for the title reaction (Table 1, entry 14). This remarkable change in the activity of Au catalyst suggests that the electronic state of Au is the most dominant factor for Au-catalyzed thioetherification. As for Au/CeO<sub>2</sub>, which showed high catalytic performance for C–S coupling, Au(III) species remained even after calcination in air at 300 °C. On the other hand, XP spectra of Au/TiO<sub>2</sub> and Au/SiO<sub>2</sub> indicated a low content of cationic Au species, suggesting that calcination in air at 300 °C was sufficient to reduce Au species on TiO<sub>2</sub> and SiO<sub>2</sub> to form metallic species. Given these XPS results as well as the fact that cationic Au complex showed high catalytic activity (Table 1, entry 12), we can surmise that supported Au catalysts which contain cationic Au species before the catalytic run functioned as an appropriate source for generating soluble and highly active cationic Au species.

Based on these considerations, we propose a possible reaction mechanism for the thioetherification of phosphates by Au catalysts. Initially, the treatment of allyl phosphates and



no activity **Scheme 6.** Possible reaction mechanism for thioetherification by Au/ZrO<sub>2</sub>.

thiosilane with Au NPs having cationic species at their surface generates soluble cationic Au species. The facts that Au cation is reported to function as soft Lewis acids which can interact with  $\pi$ -molecules, such as arenes and alkenes<sup>45,46</sup> and that aryl groups were indispensable for an efficient reaction (Scheme 5) suggest that the  $\pi$ -coordination of aryl group stabilizes the cationic Au species. Subsequently, the phosphate and alkene moieties in allyl phosphate coordinate to the Lewis acidic silyl group and the cationic Au species, respectively. This Lewis acidic activation of an allyl phosphate facilitates S–Si bond cleavage and simultaneous nucleophilic attack of allylic carbon by sulfur in an  $S_N2$  manner to give an allyl sulfide. The reaction orders for allyl phosphate and thiosilane were estimated to be  $-0.5$  and  $1.2$ , respectively. These results also support the idea that the C–S bond-forming reaction proceeds via an  $S_N2$ -type mechanism (see Supplementary Information). In this reaction, interaction of an alkene and the soft Lewis acidic nature of Au cation are key factors in activating allylic substrates. The high leaving ability of phosphate thanks to higher basicity of phosphate anion than acetate, carbonate and chloro anions would promote  $S_N2$ -type nucleophilic substitution.

## Conclusions

In summary, an efficient synthesis of allyl, benzyl and propargyl sulfides via the thioetherification of phosphates has been achieved by using supported Au catalysts. The C–S coupling reactions proceeded under mild reaction conditions and went to completion within short reaction periods. Furthermore, the present catalytic system provided a benzyl sulfide with high enantiomeric purity via effective chirality transfer. Detailed control experiments revealed that cationic Au species operated as the true active catalyst in the solution phase, and the characterization of supported Au catalysts suggested that Au NPs with cationic species at their surface played a role in generating catalytic active species. Au/ZrO<sub>2</sub> catalysts showed excellent catalytic turnover and reusability, implying that the use of Au NPs as a source of soluble gold species could be a promising way of generating gold cations with high catalytic activity. Further applications of supported Au catalysts in other synthetic reactions are currently under investigation in our laboratory.

## Experimental

### Materials

HAuCl<sub>4</sub>·3H<sub>2</sub>O and Me<sub>2</sub>AuCl were purchased from KOJIMA CHEMICALS Co., Ltd and Sigma-Aldrich, respectively. Au(en)<sub>2</sub>Cl<sub>3</sub> was synthesized as reported in the literature.<sup>47,48</sup> ZrO<sub>2</sub> (JRC-ZRO-7), CeO<sub>2</sub> (JRC-CEO-2), TiO<sub>2</sub> (JRC-TIO-15), Al<sub>2</sub>O<sub>3</sub> (Sumitomo Chemical Co., Ltd, AKP-G015; JRC-ALO-8), and SiO<sub>2</sub> (JRC-SIO-11) were obtained from the Catalysis Society of Japan. Thiosilane (**2a**) and other organic chemicals were of analytical grade and used as received without further purification. Allyl, benzyl and propargyl phosphates were synthesized from the corresponding alcohols as reported in the literature.<sup>49–52</sup>

Thiosilane (**2b–2d**) was synthesized from the corresponding thiols as reported in the literature.<sup>31</sup>

### Physical and Analytical Measurements

The products of the catalytic runs were analyzed by GC-MS (Shimadzu GCMS-QP2010, CBP-1 capillary column, i.d. 0.25 mm, length 30 m, 50–250 °C) and gas chromatography (Shimadzu GC-2014, CBP-1 capillary column, i.d. 0.25 mm, length 30 m, 50–250 °C). NMR spectra were recorded on a JMN-ECS400 (FT, 400 MHz (<sup>1</sup>H), 100 MHz (<sup>13</sup>C)) instrument. Chemical shifts ( $\delta$ ) of <sup>1</sup>H and <sup>13</sup>C{<sup>1</sup>H} NMR spectra are referenced to SiMe<sub>4</sub>. The enantiomeric purity of organic compounds was determined by HPLC analysis (JASCO EXTREMA, Daicel chiralcel OJ-H chiral column).

The physical properties of supported Au catalysts were analyzed by atomic absorption spectroscopy (AAS), nitrogen gas adsorption, TEM, XRD, and XPS. The actual contents of gold species immobilized on the supports and leached into the reaction mixture after the catalytic run were determined by AAS analysis with a SHIMADZU AA-6200. The Brunauer-Emmett-Teller (BET) specific surface area was estimated from N<sub>2</sub> isotherms obtained using a BELSORP-mini II (Microtrac MRB, Japan) at 77 K. The analyzed samples were evacuated at 573 K for 2 h prior to the measurement. HAADF-STEM images were recorded using a JEOL JEM-3200FS transmission electron microscope. The samples were prepared by depositing drops of ethanol suspensions containing small amounts of the powders onto carbon-coated copper grids (JEOL Ltd.) followed by evaporation of the ethanol in air. X-ray powder diffraction analyses were performed using Cu K $\alpha$  radiation and a one-dimensional X-ray detector (XRD: SmartLab, RIGAKU). The samples were scanned from  $2\theta = 10^\circ$  to  $70^\circ$  at a scanning rate of  $10^\circ \text{ s}^{-1}$  and a resolution of  $0.01^\circ$  or from  $2\theta = 35^\circ$  to  $40^\circ$  at a scanning rate of  $3^\circ \text{ s}^{-1}$  and a resolution of  $0.002^\circ$ . XPS analysis of the catalysts was performed using a JPS-9010 MX instrument. The spectra were measured using Mg K $\alpha$  radiation (15 kV, 400 W) in a chamber at a base pressure of  $<10^{-7}$  Pa. All spectra were calibrated using C1s (284.5 eV) as a reference.

### Preparation of Au/ZrO<sub>2</sub>, Au/CeO<sub>2</sub>, Au/TiO<sub>2</sub> and Au/Al<sub>2</sub>O<sub>3</sub> catalysts by a deposition-precipitation method

76 mL of a 2 mM aqueous solution of HAuCl<sub>4</sub> (the gold concentration in solution corresponds to a theoretical Au loading of 3wt%) was heated at 70 °C. First, the pH was adjusted to 4 by dropwise addition of aq. NaOH (0.1 M). Next, 0.97 g of support (ZrO<sub>2</sub>, CeO<sub>2</sub>, Al<sub>2</sub>O<sub>3</sub>, or TiO<sub>2</sub>) was dispersed in the solution, and the pH was readjusted to 7 with aq. NaOH. After vigorous stirring for 1 h at 70 °C, the resulting white precipitate was separated from the suspension. Prior to their use in catalytic reactions, the catalysts were calcined in air at 573 K for 1 h. The total loading amount of metal was set at 3wt%.

### Preparation of Au/SiO<sub>2</sub> catalyst by a deposition-precipitation method

An aqueous solution of Au(en)<sub>2</sub>Cl<sub>3</sub> (1 mM, 152 mL) was heated at 70 °C. The pH of the solution was first adjusted to 10 by dropwise addition of NaOH (1 M). Next, 0.97 g of support

(Nb<sub>2</sub>O<sub>5</sub> or SiO<sub>2</sub>) was dispersed in the solution, and the pH was readjusted to 10 with NaOH. After vigorous stirring for 2 h at 70 °C, the resulting purple precipitate was separated from the suspension. Prior to their use in catalytic reactions, the catalysts were calcined in air at 300 °C for 1 h. The total loading amount of metal was set at 3wt%.

#### Preparation of ZrO<sub>2</sub>-supported metal NPs catalysts by an impregnation method

ZrO<sub>2</sub>-supported metal (Ag, Cu, Pd, Rh or Pt) catalysts were prepared by an impregnation method with the use of AgNO<sub>3</sub>, Cu(NO<sub>3</sub>)<sub>2</sub>, PdCl<sub>2</sub>, RhCl<sub>3</sub>, or H<sub>2</sub>PtCl<sub>6</sub> as a metal precursor. ZrO<sub>2</sub> was added to an aqueous solution of the metal precursor, and the suspension was stirred at 80 °C for 2 h. After the evaporation of water, the resulting powder was calcined in air at 400 °C for 3 h. The total loading amount of metal was set at 3wt%.

#### General procedure for the thioetherification of phosphate over supported Au catalyst

A typical reaction procedure for the thioetherification of phosphate is as follows: phosphate (0.3 mmol), thiosilane (0.6 mmol) and 1,4-dioxane (1.0 mL) were added to a Schlenk tube containing the supported Au catalyst (2 mol % as Au relative to phosphate) under an Ar atmosphere. The progress of the reaction was monitored by GC analysis using biphenyl as an internal standard. For isolation of the products, the solid catalyst was removed by filtration. The remaining solution was concentrated under reduced pressure and purified through silica gel column chromatography (a mixture of hexane and ethyl acetate) to give the product.

#### General procedure for reusing Au/ZrO<sub>2</sub> catalyst (Fig. 1).

After the reaction of **1a** and **2a** (Fig. 1), the solid was separated from the reaction mixture by centrifugation and completely washed three times with 10 mL of methanol. The resulting solid was dried for 1 h at 80 °C under a reduced pressure (< 0.1 Torr) to give the Au/ZrO<sub>2</sub> catalyst for reuse.

#### General procedure for hot filtration tests (Fig. 2).

A 20 mL Schlenk tube was charged with **1a** and **2a**, Au/ZrO<sub>2</sub> catalyst, and 1,4-dioxane (1.0 mL) under an argon atmosphere. After the reaction was allowed to proceed for 15 min at 35 °C, through a 0.45 μm syringe filter (Millipore Millex LH) into another preheated Schlenk tube. The filtrate was stirred at 35 °C. The conversion and yields of the product after filtration were followed by GC and GC-MS analyses. The results are shown in Fig. 2.

#### Conflicts of interest

There are no conflicts of interest to declare.

#### Acknowledgements

This study was supported in part by the Program for Element Strategy Initiative for Catalysts & Batteries (ESICB) (Grant

JPMXP0112101003), JST FOREST Program (Grant JPMJFR203V), and Grants-in-Aid for Scientific Research (B) (Grant 21H01719), Early-Career Scientists (Grant 19K15362) and Scientific Research on Innovative Areas (Grant 17H06443) commissioned by MEXT of Japan. We wish to thank Mr. Ono of Tokyo Metropolitan University for providing valuable technical support during the HAADF-TEM observations.

#### Notes and references

- 1 N. Wang, P. Saidharedy and X. Jiang, *Nat. Prod. Rep.*, 2020, **37**, 246–275.
- 2 T. Kondo and T. Mitsudo, *Chem. Rev.*, 2000, **100**, 3205–3220.
- 3 I. P. Beletskaya and V. P. Ananikov, *Chem. Rev.*, 2011, **111**, 1596–1636.
- 4 W. Liu and X. Zhao, *Synthesis*, 2013, **45**, 2051–2069.
- 5 P. Chauhan, S. Mahajan and D. Enders, *Chem. Rev.*, 2014, **114**, 8807–8864.
- 6 J.-S. Yu, H.-M. Huang, P.-G. Ding, X.-S. Hu, F. Zhou and J. Zhou, *ACS Catal.*, 2016, **6**, 5319–5344.
- 7 K. L. Dunbar, D. H. Scharf, A. Litomska and C. Hertweck, *Chem. Rev.*, 2017, **117**, 5521–5577.
- 8 Y. A. Lin, J. M. Chalker, N. Floyd, G. J. L. Bernardes and B. G. Davis, *J. Am. Chem. Soc.*, 2008, **130**, 9642–9643.
- 9 S. A. Vizer, E. S. Sycheva, A. A. A. Al Quntar, N. B. Kurmankulov, K. B. Yerzhanov and V. M. Dembitsky, *Chem. Rev.*, 2015, **115**, 1475–1502.
- 10 I. Colomer, M. Velado, R. Fernández de la Pradilla and A. Viso, *Chem. Rev.*, 2017, **117**, 14201–14243.
- 11 A. Saha and B. C. Ranu, *Tetrahedron Lett.*, 2010, **51**, 1902–1905.
- 12 R. A. Croft, J. J. Mousseau, C. Choi and J. A. Bull, *Chem. - Eur. J.*, 2018, **24**, 818–821.
- 13 M. Jegelka and B. Plietker, *Org. Lett.*, 2009, **11**, 3462–3465.
- 14 K. Venkatesham, C. Bhujanga Rao, C. B. Dokuburra, R. A. Bunce and Y. Venkateswarlu, *J. Org. Chem.*, 2015, **80**, 11611–11617.
- 15 Y. Yatsumonji, Y. Ishida, A. Tsubouchi and T. Takeda, *Org. Lett.*, 2007, **9**, 4603–4606.
- 16 T. Kondo, Y. Morisaki, S. Uenoyama, K. Wada and T. Mitsudo, *J. Am. Chem. Soc.*, 1999, **121**, 8657–8658.
- 17 T. Kondo, Y. Kanda, A. Baba, K. Fukuda, A. Nakamura, K. Wada, Y. Morisaki and T. Mitsudo, *J. Am. Chem. Soc.*, 2002, **124**, 12960–12961.
- 18 Y. Inada, Y. Nishibayashi, M. Hidai and S. Uemura, *J. Am. Chem. Soc.*, 2002, **124**, 15172–15173.
- 19 S. Tanaka, P. K. Pradhan, Y. Maegawa and M. Kitamura, *Chem. Commun.*, 2010, **46**, 3996.
- 20 A. B. Zaitsev, H. F. Caldwell, P. S. Pregosin and L. F. Veiros, *Chem. - Eur. J.*, 2009, **15**, 6468–6477.
- 21 B. M. Trost and T. S. Scanlan, *Tetrahedron Lett.*, 1986, **27**, 4141–4144.
- 22 C. Goux, P. Lhoste and D. Sinou, *Tetrahedron Lett.*, 1992, **33**, 8099–8102.
- 23 Y. Arredondo, M. Moreno-Mañas, R. Pleixats and M. Villarroya, *Tetrahedron*, 1993, **49**, 1465–1470.
- 24 C. Goux, P. Lhoste and D. Sinou, *Tetrahedron*, 1994, **50**, 10321–10330.
- 25 M. Frank and H.-J. Gais, *Tetrahedron Asymmetry*, 1998, **9**, 3353–3357.
- 26 H.-J. Gais, N. Spalthoff, T. Jagusch, M. Frank and G. Raabe, *Tetrahedron Lett.*, 2000, **41**, 3809–3812.

- 27 K. J. Miller and M. M. Abu-Omar, *Eur. J. Org. Chem.*, 2003, **2003**, 1294–1299.
- 28 T. Itoh and T. Mase, *Org. Lett.*, 2004, **6**, 4587–4590.
- 29 T. Schlatzer, J. Kriegesmann, H. Schröder, M. Trobe, C. Lembacher-Fadum, S. Santner, A. V. Kravchuk, C. F. W. Becker and R. Breinbauer, *J. Am. Chem. Soc.*, 2019, **141**, 14931–14937.
- 30 T. Schlatzer, H. Schröder, M. Trobe, C. Lembacher-Fadum, S. Stangl, C. Schlögl, H. Weber and R. Breinbauer, *Adv. Synth. Catal.*, 2020, **362**, 331–336.
- 31 Y. Nishimoto, A. Okita, M. Yasuda and A. Baba, *Org. Lett.*, 2012, **14**, 1846–1849.
- 32 T. Miyazaki, S. Kasai, Y. Ogiwara and N. Sakai, *Eur. J. Org. Chem.*, 2016, **2016**, 1043–1049.
- 33 S. Zheng, N. Gao, W. Liu, D. Liu, X. Zhao and T. Cohen, *Org. Lett.*, 2010, **12**, 4454–4457.
- 34 N. Gao, S. Zheng, W. Yang and X. Zhao, *Org. Lett.*, 2011, **13**, 1514–1516.
- 35 M. Roggen and E. M. Carreira, *Angew. Chem. Int. Ed.*, 2012, **51**, 8652–8655.
- 36 L. Herkert, S. L. J. Green, G. Barker, D. G. Johnson, P. C. Young, S. A. Macgregor and A.-L. Lee, *Chem. - Eur. J.*, 2014, **20**, 11540–11548.
- 37 K. Ohta, E. Koketsu, Y. Nagase, N. Takahashi, H. Watanabe and M. Yoshimatsu, *Chem. Pharm. Bull.*, 2011, **59**, 1133–1140.
- 38 A. Corma and H. Garcia, *Chem. Soc. Rev.*, 2008, **37**, 2096.
- 39 H. Miura, R. Hirata, T. Tomoya and T. Shishido, *ChemCatChem*, 2021, **13**, 4705–4713.
- 40 H. Miura, Y. Hachiya, H. Nishio, Y. Fukuta, T. Toyomasu, K. Kobayashi, Y. Masaki and T. Shishido, *ACS Catal.*, 2021, **11**, 758–766.
- 41 M. Haruta, *Chem. Rec.*, 2003, **3**, 75–87.
- 42 H. H. Morris, *J. Am. Chem. Soc.*, 1918, **40**, 917–927.
- 43 I. V. Mironov and L. D. Tsvlodub, *Russ. J. Inorg. Chem.*, 2000, **45**, 633–637.
- 44 M. A. Macchione, J. E. Samaniego, R. Moiraghi, N. Passarelli, V. A. Macagno, E. A. Coronado, M. J. Yacaman and M. A. Pérez, *RSC Adv.*, 2018, **8**, 19979–19989.
- 45 J. Rodriguez, G. Szalóki, E. D. S. Carrizo, N. Saffon-Merceron, K. Miqueu, D. Bourissou, *Angew. Chem. Int. Ed.* 2020, **59**, 1511–1515.
- 46 R. Zanella, A. Sandoval, P. Santiago, V. A. Basiuk and J. M. Saniger, *J. Phys. Chem. B*, 2006, **110**, 8559–8565.
- 47 H. Zhu, Z. Ma, J. C. Clark, Z. Pan, S. H. Overbury and S. Dai, *Appl. Catal. Gen.*, 2007, **326**, 89–99.
- 48 M. Hojo, R. Sakuragi, S. Okabe and A. Hosomi, *Chem. Commun.*, 2001, 357–358.
- 49 H. Ohmiya, Y. Makida, D. Li, M. Tanabe and M. Sawamura, *J. Am. Chem. Soc.*, 2010, **132**, 879–889.
- 50 H. Ohmiya, U. Yokobori, Y. Makida and M. Sawamura, *Org. Lett.*, 2011, **13**, 6312–6315.
- 51 S. S. M. Spoehrle, T. H. West, J. E. Taylor, A. M. Z. Slawin and A. D. Smith, *J. Am. Chem. Soc.*, 2017, **139**, 11895–11902.
- 52 B. Wang, X. Wang, X. Yin, W. Yu, Y. Liao, J. Ye, M. Wang and J. Liao, *Org. Lett.*, 2019, **21**, 3913–3917.